

# UC Berkeley

## UC Berkeley Previously Published Works

### Title

Chemical Vapor Deposition of Phase-Pure Uranium Dioxide Thin Films from Uranium(IV) Amidate Precursors

### Permalink

<https://escholarship.org/uc/item/9z1611rs>

### Journal

Angewandte Chemie, 131(17)

### ISSN

0044-8249

### Authors

Straub, Mark D  
Leduc, Jennifer  
Frank, Michael  
et al.

### Publication Date

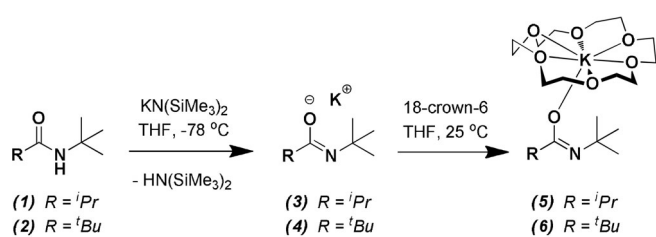
2019-04-16

### DOI

10.1002/ange.201901924

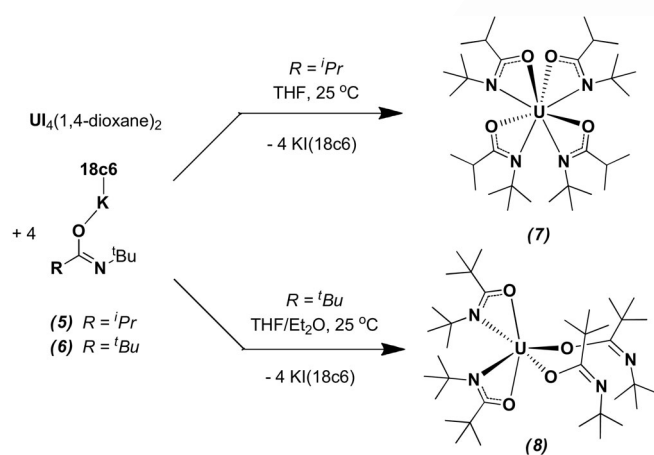
Peer reviewed





**Scheme 1.** Synthesis of the crowned potassium amidates K(ITA) (18c6) (5) and K(TTA) (18c6) (6).

The homoleptic amidate complexes  $U(ITA)_4$  (**7**) and  $U(TTA)_4$  (**8**) were synthesized by treating  $U(1,4\text{-dioxane})_2$  with four equivalents of **5** or **6**, respectively (Scheme 2). We also synthesized **7** and **8** via a protonolysis route with  $[(Me_3Si)_2N]_2U[\kappa^2\text{-}(C,N)\text{-}CH_2Si(Me)_2N(SiMe_3)]$  and **1** or **2**, but yields were lower using this method. Green crystals of **7** and teal crystals of **8** suitable for X-ray diffraction were grown from  $Et_2O$  and pentane, respectively.



**Scheme 2.** Synthesis of  $U(ITA)_4$  (**7**) and  $U(TTA)_4$  (**8**).

Although the proligands **1** and **2** are sterically comparable, we observed different molecular geometries for **7** and **8**. Crystallographic analysis of **7** showed this molecule to be eightfold coordinated and  $D_{2d}$ -symmetric, with all four amidate ligands chelated ( $\kappa_2\text{-}N,O$ ) to the uranium center. By comparison, **8** is sixfold coordinated and  $C_1$ -symmetric, with two ( $\kappa_2\text{-}N,O$ ) amidate ligands and two ( $\kappa_1\text{-}O$ ) amidate ligands bound to the uranium center. This difference in geometry can possibly be attributed to the higher electron-donating effect of the *tert*-butyl vs. *iso*-propyl substituents on the amidate backbone, disfavoring electron donation from the lone pairs on all four nitrogen atoms to the uranium center in **8**; however, it is also possible that the larger steric bulk of the  $C\text{-}tBu$  substituent contributes to the lower coordination number of **8**.

The  $U\text{-}O$  and  $U\text{-}N$  bond lengths (Table 1) in **7** are comparable to the analogous  $U\text{-}O$  and  $U\text{-}N$  bonds of the chelated amidates in **8** (2.284(4) and 2.296(4) Å for  $U\text{-}O$ ). However, the  $U\text{-}O$  bonds of the  $O$ -bound amidates in **8** are substantially shorter (2.123(5) and 2.135(4) Å), suggesting an

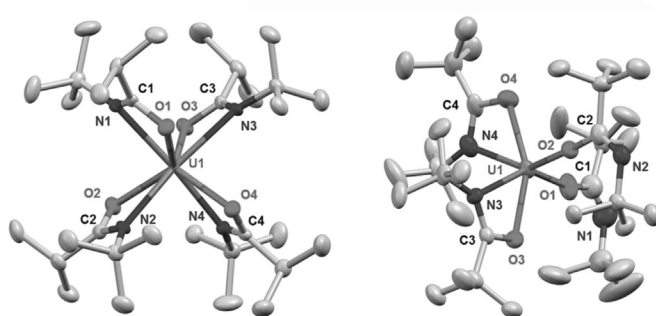


**Figure 1.** 50% probability thermal ellipsoid view of  $U(ITA)_4$  (**7**) (left) and  $U(TTA)_4$  (**8**) (right). Hydrogen atoms are omitted for clarity.

**Table 1:** Selected bond lengths in **7** and **8**.

Atoms	Bond lengths (Å)	
	<b>7</b>	<b>8</b>
$U1\text{-}O1$	2.333(2)	2.123(5)
$U1\text{-}O2$	2.350(2)	2.135(4)
$U1\text{-}O3$	2.366(2)	2.284(4)
$U1\text{-}O4$	2.346(2)	2.296(4)
$U1\text{-}N1$	2.499(3)	–
$U1\text{-}N2$	2.507(2)	–
$U1\text{-}N3$	2.502(2)	2.495(5)
$U1\text{-}N4$	2.493(3)	2.457(5)
$C1\text{-}O1$	1.307(4)	1.375(9)
$C2\text{-}O2$	1.311(3)	1.361(7)
$C3\text{-}O3$	1.296(4)	1.323(7)
$C4\text{-}O4$	1.303(4)	1.323(7)
$C1\text{-}N1$	1.305(4)	1.141(11)
$C2\text{-}N2$	1.292(4)	1.240(9)
$C3\text{-}N3$	1.296(4)	1.297(8)
$C4\text{-}N4$	1.310(4)	1.309(9)

increased localization of electron density on the oxygen atoms of these ligands when bound  $\kappa_1\text{-}O$ . Providing further support for this claim, the  $O$ -bound ligands in **8** also possess longer  $C\text{-}O$  bonds (1.375(9) and 1.361(7) Å) and shorter  $C\text{-}N$  bonds (1.141(11) and 1.240(9) Å for  $C\text{-}N$ ) than their chelated counterparts (1.323(7) and 1.323(7) Å for  $C\text{-}O$ ; 1.297(8) and 1.309(9) Å).

The thermal decomposition of the precursors was further investigated using thermogravimetric (TG) analysis (Figure 2). Precursor **7** showed an onset of decomposition at 85°C, while precursor **8** showed it at 70°C. The experimentally detected overall weight losses of **7** (65.0%) and **8** (62.7%) are lower than the theoretical values of 66.5% and

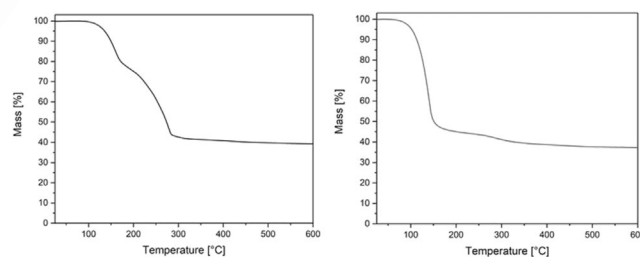


**Figure 2.** Thermograms of **7** (left) and **8** (right) collected under nitrogen at a heating rate of  $5^\circ\text{C min}^{-1}$ .

68.8% for the formation of  $\text{UO}_2$ , suggesting a potential incorporation of carbon impurities; this mass difference is substantially more prominent for precursor **7** than for precursor **8**. An in-depth discussion on the TG analysis can be found in the Supporting Information.

To elucidate the decomposition mechanism of these precursors to uranium oxide, solid samples of **7** and **8** were heated to 300 °C in sealed J-Young tubes under a nitrogen atmosphere. The tubes were then cooled with liquid nitrogen to condense volatile decomposition products, and  $\text{C}_6\text{D}_6$  was added for NMR analysis. Three main products were visible in the resulting  $^1\text{H}$  NMR spectra of the decomposed precursors: the amides **1** or **2**, isobutyronitrile (from **7**) or pivalonitrile (from **8**), and isobutylene. A small amount of insoluble black uranium oxide precipitate was also observed. These products are consistent with an alkene elimination mechanism (Scheme 3), as reported previously for related homoleptic  $\text{Zr}^{\text{IV}}$  amidates.<sup>[26]</sup> We also observed slow formation of the same products by heating solutions of **7** and **8** to 150 °C in  $[\text{D}_8]\text{toluene}$  over the course of multiple days.

In the first decomposition step, isobutylene elimination from a nitrogen atom generates a hemiamidate intermediate (**D-1**). This hemiamidate then undergoes protonolysis with another amidate ligand to promote the elimination of one equivalent each of amide and nitrile, leaving an oxygen atom bound to the uranium center (**D-2**). Because this is a low-coordinate system, it is likely that the intermediate **D-2** aggregates prior to the elimination of additional ligands. A second iteration of this process yields  $\text{UO}_2$  and one more equivalent each of isobutylene, amide, and nitrile.

Complexes **7** and **8** were both tested as  $\text{UO}_2$  thin film precursors in a cold-wall thermal CVD reactor. We were interested to determine if the oxidation state of the precursors would be retained in the CVD-generated materials to form stoichiometric  $\text{UO}_2$  films, as suggested by the thermal decomposition experiments. Since the sublimation temperatures and decomposition temperatures at a pressure of  $10^{-3}$  mbar were in very close vicinity ( $\approx 130^\circ\text{C}$  for **7**,  $\approx 120^\circ\text{C}$  for **8**), CVD experiments were performed at a pressure of  $10^{-6}$  mbar to favor sublimation of the precursors. To ensure a proper precursor flow, the precursor temperatures were set to 160 °C. Since TG analysis displayed a complete decomposition of both precursors at a temperature of 500 °C, substrate temperatures of 500 °C were chosen for both CVD processes. Precursor **7** sublimed without prior decomposition in the precursor flask, and black films were generated during

the CVD process. In contrast, the deposition process using complex **8** was not successful; we postulate that this may be due to the weakly bound  $\kappa_1$ -O-coordinated ligands and thus a thermal instability of the precursor.

Following the deposition process, the films were characterized without an additional annealing step to determine if  $\text{UO}_2$  was prepared directly. As shown by XPS (Figure 3) and XRD (Figure 4) analyses, the film surface and the bulk are composed of phase-pure  $\text{UO}_2$ . This finding is noteworthy given the pronounced tendency of uranium dioxide to exhibit surface oxidation, resulting in hyperstoichiometric compositions ( $\text{O}:\text{U} > 2:1$ ). The XPS survey spectrum exhibited signals attributable solely to uranium, oxygen, and carbon (Figure 3, left). The high-resolution U 4f XPS spectrum showed two main signals at 380.4 eV and 391.4 eV, corresponding to the  $\text{U } 4f_{7/2}$  and  $\text{U } 4f_{5/2}$  orbitals, respectively (Figure 3, bottom). The peak positions of the main signals and the satellites (binding-energy distance to the main signals of  $\text{DE}_{\text{sat}} = 6.9$  eV) are consistent with the reported data.<sup>[5]</sup> The Bragg

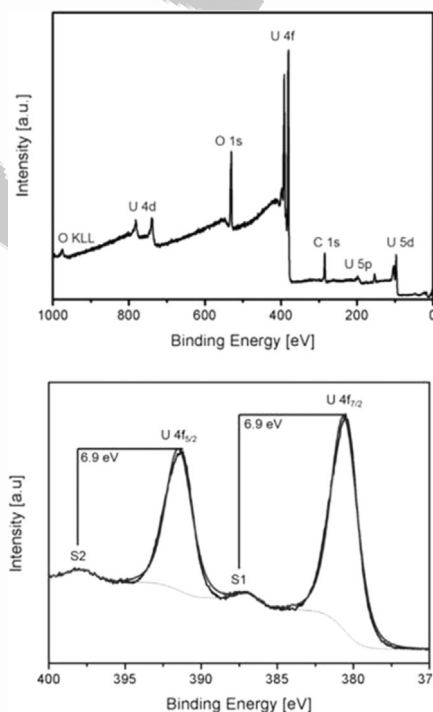
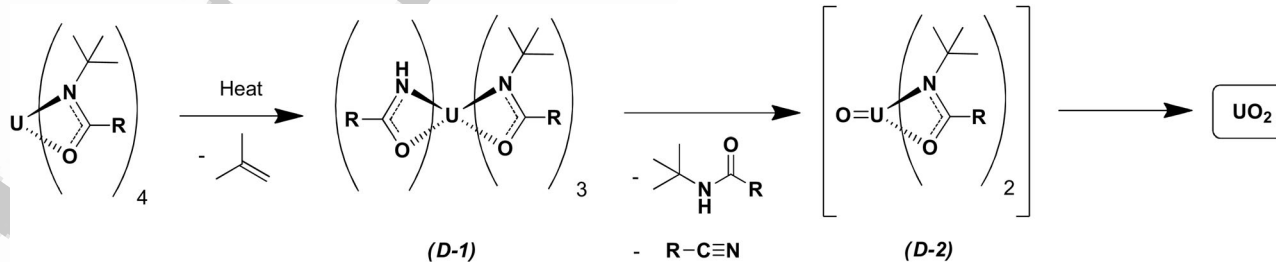


**Figure 3.** XPS survey spectrum (top) and high-resolution U 4f XPS spectrum (bottom) of crystalline  $\text{UO}_2$  films prepared via CVD using **7**.



**Scheme 3.** Proposed decomposition mechanism of **7** and **8**. Alkene, amide, and nitrile byproducts were observed by NMR; intermediate decomposition products **D-1** and **D-2** are postulated.

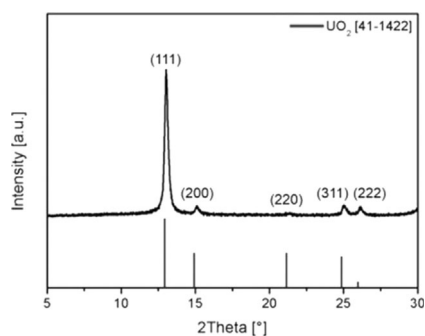


**Figure 4.** Powder XRD pattern of the film deposited using **7** at a precursor temperature of 160 °C and a substrate temperature of 500 °C.

reflections in the XRD pattern were assigned to cubic fluorite-type  $\text{UO}_2$  (Figure 4). The peaks at  $2\theta = 13.0^\circ$ ,  $15.0^\circ$ ,  $21.2^\circ$ ,  $24.9^\circ$ , and  $26.0^\circ$  were indexed to the (111), (200), (220), (311), and (222) planes, respectively. Since the diffraction peaks are broadened anisotropically, the crystallite sizes were calculated using the Scherrer equation and amounted to 146 nm, 195 nm, and 99 nm for the (111)/(222), (200), and (311) planes, respectively. Although the anisotropic broadening suggests the formation of anisotropic crystallite shapes, the predominant intensity of the reflection indexed to the (111) plane hints towards a preferred growth direction that was confirmed by the surface topography (Figure 5). Taken together, these results strongly suggest that phase-pure  $\text{UO}_2$  films were prepared directly via decomposition of the molecular precursor.

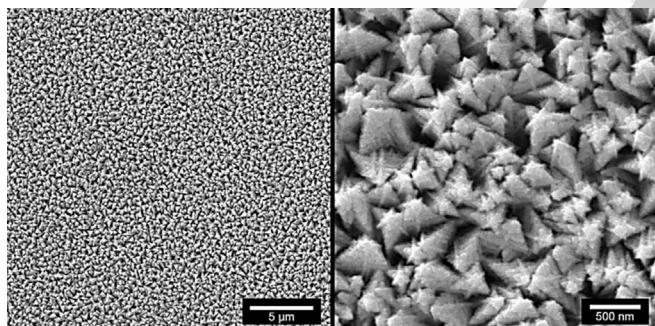


**Figure 5.** Top-view SEM images with different magnifications of crystalline  $\text{UO}_2$  films, prepared via CVD from precursor **7**.

The vapor-deposited  $\text{UO}_2$  films exhibited a homogeneous distribution of fir tree-like structures at the surface and good adhesion to the silicon substrate, as depicted in the top-view (Figure 5) and side-view (Figure 6) SEM images, respectively. The side-view SEM images additionally revealed the formation of a dense layer with a thickness of  $\approx 400$  nm at the substrate interface, which seamlessly continues into a branch-like structure with a thickness of  $\approx 2.5$   $\mu\text{m}$ . This change in the microstructure from 2D to 1D growth is likely due to the good lattice match between silicon ( $a = 5.431$  Å) and  $\text{UO}_2$  ( $a = 5.471$  Å), which facilitates epitaxial growth of  $\text{UO}_2$  onto Si

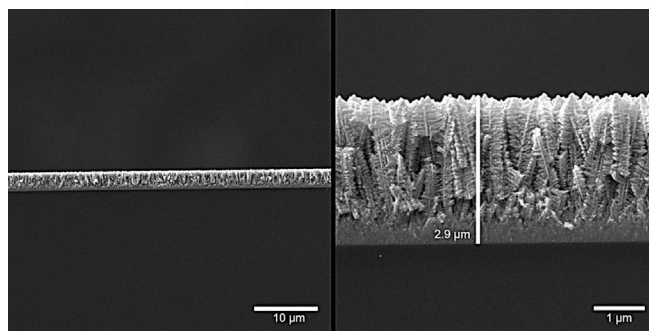


**Figure 6.** Side-view SEM images with different magnifications of crystalline  $\text{UO}_2$  films, prepared via CVD from precursor **7**. The thickness of these films is 2.9  $\mu\text{m}$ .

up to a thickness of about 400 nm. Beyond this thickness, the cubic  $\text{UO}_2$  crystals act as seeds for 1D nanostructures that grow with equal probability in multiple directions, leading to the formation of branch-like structures.

In summary, we have developed an effective single-source route to fabricate crystalline, phase-pure  $\text{UO}_2$  films through chemical vapor deposition of  $\text{U}^{\text{IV}}$  amidate molecular precursors, which decompose cleanly via alkene elimination. Small changes in the ligand substituents were seen to affect both the molecular geometry and the decomposition behavior of the precursors, with the eightfold coordinated complex **7** performing much more favorably in thin-film deposition than the sixfold coordinated complex **8**. XRD and XPS measurements confirmed the vapor-deposited uranium oxide films to be stoichiometric  $\text{UO}_2$ , and SEM images showed good epitaxial growth of the  $\text{UO}_2$  layer on the Si substrate. Above a film thickness of about 400 nm, the  $\text{UO}_2$  crystals formed fir tree-like structures with an isotropic growth of 1D branches and a large accessible surface area. Given the anisotropic microstructure and high surface area of these films in conjunction with high charge-carrier mobilities in  $\text{UO}_2$ , we plan to investigate the performance of these films as photoanodes in photoelectrochemical water splitting reactions.

### Acknowledgements

This work was supported by the Director, Office of Science, Office of Basic Energy Sciences, Division of Chemical Sciences, Geosciences, and Biosciences Heavy Element Chemistry Program of the U.S. Department of Energy (DOE) at LBNL under Contract No. DE-AC02-05CH11231. The Advanced Light Source (ALS) is supported by the Director, Office of Science, Office of Basic Energy Sciences, of the U.S. Department of Energy under Contract No. DE-AC02-05CH11231. We thank Dr. Simon J. Teat for oversight of our crystallographic studies at the ALS. We also thank M. A. Boreen, N. S. Settineri, and L. M. Moreau for helpful discussions. J.L., M.F., A.R. and S.M. thank the University of Cologne for providing infrastructural support. J.L. thanks the Fonds der Chemischen Industrie for a PhD fellowship. A.R. acknowledges the DAAD for a travel grant. The financial support in the framework of the DFG priority

1 programs SPP 1613 “Fuels Produced Regeneratively Through  
2 Light-Driven Water Splitting: Clarification of the Elemental  
3 Processes Involved and Prospects for Implementation in  
4 Technological Concepts” and SPP 1959 “Manipulation of  
5 matter controlled by electric and magnetic field: Towards  
6 novel synthesis and processing routes of inorganic materials”  
7 are gratefully acknowledged.

### 8 9 10 Conflict of interest

11 The authors declare no conflict of interest.

12  
13 **Keywords:** Actinides · Chemical vapor deposition ·  
14 Inorganic materials · Thin films · Uranium

- 
- 15  
16  
17  
18  
19  
20 [1] S. J. Zinkle, G. S. Was, *Acta Mater.* **2013**, *61*, 735–758.  
21 [2] S. J. Zinkle, K. A. Terrani, J. C. Gehin, L. J. Ott, L. L. Snead, *J.*  
22 *Nucl. Mater.* **2014**, *448*, 374–379.  
23 [3] K. Nogita, K. Une, *J. Nucl. Mater.* **1997**, *250*, 244–249.  
24 [4] S. R. Qiu, C. Amrhein, M. L. Hunt, R. Pfeffer, B. Yakshinskiy, L.  
25 Zhang, T. E. Madey, J. A. Yarmoff, *Appl. Surf. Sci.* **2001**, *181*,  
26 211–224.  
27 [5] H. Idriss, *Surf. Sci. Rep.* **2010**, *65*, 67–109.  
28 [6] T. T. Meek, B. Von Roedern, P. G. Clem, R. J. Hanrahan, *Mater.*  
29 *Lett.* **2005**, *59*, 1085–1088.  
30 [7] T. S. Noggle, J. O. Stiegler, *J. Appl. Phys.* **1960**, *31*, 2199–2208.  
31 [8] Q. Chen, X. Lai, B. Bai, M. Chu, *Appl. Surf. Sci.* **2010**, *256*, 3047–  
32 3050.  
33 [9] J. Lin, I. Dahan, B. Valderrama, M. V. Manuel, *Appl. Surf. Sci.*  
34 **2014**, *301*, 475–480.  
35 [10] M. M. Strehle, B. J. Heuser, M. S. Elbakhshwan, X. Han, D. J.  
36 Gennardo, H. K. Pappas, H. Ju, *Thin Solid Films* **2012**, *520*,  
37 5616–5626.  
38 [11] R. J. McEachern, P. Taylor, *J. Nucl. Mater.* **1998**, *254*, 87–121.  
39 [12] A. K. Burrell, T. M. McCleskey, P. Shukla, H. Wang, T.  
40 Durakiewicz, D. P. Moore, C. G. Olson, J. J. Joyce, Q. Jia, *Adv.*  
41 *Mater.* **2007**, *19*, 3559–3563.

- 1  
2  
3  
4  
5  
6  
7  
8  
9  
10  
11  
12  
13  
14  
15  
16  
17  
18  
19  
20  
21  
22  
23  
24  
25  
26  
27  
28  
29  
30  
31  
32  
33  
34  
35  
36  
37  
38  
39  
40  
41  
42  
43  
44  
45  
46  
47  
48  
49  
50  
51  
52  
53  
54  
55  
56  
57  
58  
59
- [13] B. L. Scott, J. J. Joyce, T. D. Durakiewicz, R. L. Martin, T. M. McCleskey, E. Bauer, H. Luo, Q. Jia, *Coord. Chem. Rev.* **2014**, *266–267*, 137–154.  
[14] H. Pierson, *Handbook of Chemical Vapor Deposition (CVD)*, **1999**. ■ ■ publisher and city missing ■ ■  
[15] S. T. Barry, *Coord. Chem. Rev.* **2013**, *257*, 3192–3201.  
[16] F. T. Edelmann, *Chem. Soc. Rev.* **2012**, *41*, 7657–7672. ■ ■ page numbers ok? ■ ■  
[17] B. S. Lim, A. Rahtu, J.-S. Park, R. G. Gordon, *Inorg. Chem.* **2003**, *42*, 7951–7958.  
[18] T. B. Thiede, M. Krasnopolski, A. P. Milanov, T. de los Arcos, A. Ney, H.-W. Becker, D. Rogalla, J. Winter, A. Devi, R. A. Fischer, *Chem. Mater.* **2011**, *23*, 1430–1440.  
[19] M. Gebhard, M. Hellwig, A. Kroll, D. Rogalla, M. Winter, B. Mallick, A. Ludwig, M. Wiesing, A. D. Wiecek, G. Grundmeier, et al., *Dalton Trans.* **2017**, *38*, 819.  
[20] R. C. Smith, T. Ma, N. Hoilien, L. Y. Tsung, M. J. Bevan, L. Colombo, J. Roberts, S. A. Campbell, W. L. Gladfelter, *Adv. Mater. Opt. Electron.* **2000**, *10*, 105–114.  
[21] Y. Shi, L. Li, *Chem. Soc. Rev.* **2015**, *44*, 2744–2756.  
[22] C. H. Winter, P. H. Sheridan, T. S. Lewkebandara, M. J. Heeg, J. W. Proscialc, *J. Am. Chem. Soc.* **1992**, *114*, 1095–1097.  
[23] Y. Shiokawa, R. Amano, A. Nomura, M. Yagi, *J. Radioanal. Nucl. Chem.* **1991**, *152*, 373–380.  
[24] L. Appel, J. Leduc, C. L. Webster, J. W. Ziller, W. J. Evans, S. Mathur, *Angew. Chem. Int. Ed.* **2015**, *54*, 2209–2213; *Angew. Chem.* **2015**, *127*, 2237–2241.  
[25] M. D. Straub, S. Hohloch, S. G. Minasian, J. Arnold, *Dalton Trans.* **2018**, *47*, 1772–1776.  
[26] A. L. Catherall, M. S. Hill, A. L. Johnson, G. Kociok-Köhn, M. F. Mahon, *J. Mater. Chem. C* **2016**, *4*, 10731–10739.  
[27] T. Perera, Wayne State University Dissertation, **2012**.  
[28] M. C. Karunaratne, J. W. Baumann, M. J. Heeg, P. D. Martin, C. H. Winter, *J. Organomet. Chem.* **2017**, *847*, 204–212.  
[29] C. Li, R. K. Thomson, B. Gillon, B. O. Patrick, L. L. Schafer, *Chem. Commun.* **2003**, 2462.

Manuscript received: February 13, 2019

Accepted manuscript online: February 28, 2019

Version of record online: ■ ■ ■ ■, ■ ■ ■ ■

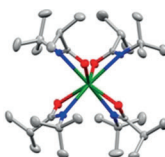
## Communications

## Uranium Chemistry

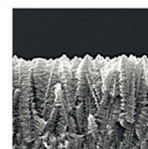
M. D. Straub, J. Leduc, M. Frank,  
A. Rauf, T. D. Lohrey, S. G. Minasian,  
S. Mathur,\* J. Arnold\* — ■■■■—■■■■

Chemical Vapor Deposition of Phase-Pure  
Uranium Dioxide Thin Films from  
Uranium(IV) Amidate Precursors

U(IV) molecular  
precursor



CVD



Uranium dioxide  
nano-forest

**Uranium deposit:** Volatile uranium(IV)  
amidate complexes are used as single-  
source molecular precursors to uranium  
oxide films. Chemical vapor deposition

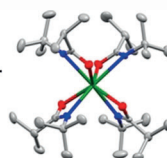
(CVD) of these single-source precursors  
yields crystalline, phase-pure  $\text{UO}_2$  films  
with a fir tree-like microstructure and  
a high surface area.

## Uranchemie

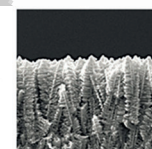
M. D. Straub, J. Leduc, M. Frank,  
A. Rauf, T. D. Lohrey, S. G. Minasian,  
S. Mathur,\* J. Arnold\* — ■■■■—■■■■

Chemical Vapor Deposition of Phase-Pure  
Uranium Dioxide Thin Films from  
Uranium(IV) Amidate Precursors

molekularer U(IV)-  
Precursor



CVD



Urandioxid-  
Nanowald

**Oh Tannenbaum, Uran-Tannenbaum:**  
Flüchtige Uran(IV)-Amidatkomplexe  
werden als molekulare Präkursoren zur  
Abscheidung von Uranoxidfilmen ge-  
nutzt. Die chemische Gas-

phasenabscheidung (CVD) dieser Prä-  
kursoren ergibt kristalline, phasenreine  
 $\text{UO}_2$ -Filme mit einer tannenbaumartigen  
Mikrostruktur und großen Oberfläche.

Please check that the ORCID identifiers listed below are correct. We encourage all authors to provide an ORCID identifier for each coauthor. ORCID is a registry that provides researchers with a unique digital identifier. Some funding agencies recommend or even require the inclusion of ORCID IDs in all published articles, and authors should consult their funding agency guidelines for details. Registration is easy and free; for further information, see <http://orcid.org/>.

Mark D. Straub  
Jennifer Leduc  
Michael Frank  
Aida Rauf  
Trevor D. Lohrey  
Stefan G. Minasian  
Prof. Dr. Sanjay Mathur  
Prof. Dr. John Arnold <http://orcid.org/0000-0001-9671-227X>